

# Experimental investigations of correlation phenomena in the relaxation of velocity-spread beam in a plasma

S. M. Krivoruchko, V. A. Bashko, and A. S. Bakaĭ

*Kharkov Physicotechnical Institute, Ukrainian Academy of Sciences*

(Submitted 1 July 1980)

Zh. Eksp. Teor. Fiz. **80**, 579–581 (February 1981)

Results are presented of an experimental investigation of the manifestation of field correlation and particle motion in a relaxing electron beam with large initial velocity spread. The investigations are made in a wide range of beam currents and with introduction of weak initial field correlations in the form of monochromatic oscillations and short wave trains. The mechanism of wave interaction via resonant particles, which leads to the observed correlation phenomena, is studied. A comparison of the experimental results with the main predictions of the quasilinear theory and of the theory of moderate turbulence corroborates the validity of the latter.

PACS numbers: 52.40.Mj

## INTRODUCTION

Correlation phenomena in resonant interaction of waves and particles, particularly in the relaxation of a weak electron beam having a large velocity spread in a plasma, are presently the subject of intensive study in plasma theory. It was pointed out in a number of papers<sup>1-4</sup> that the time of loss of pair correlation of particle motion can turn out to be quite long compared with the beam correlation time if the initial particle velocities and coordinates do not differ greatly. This leads to formation of long-lived macroparticles, to granulation (spatial and velocity inhomogeneity of the distribution function, and to deviations from a quasilinear relaxation process.<sup>5,6</sup> The correlation properties of particle motion in a field was analyzed somewhat later also by Misquich and Balescu.<sup>7</sup>

It was shown in a number of papers,<sup>8-12</sup> theoretically as well as by numerical modeling, that field correlations and particle-motion correlations appear in a relaxing beam when the characteristic time  $\tau_{NL}$  of interaction of the waves and particles becomes shorter than the quasilinear relaxation time  $\tau_{QL}$ . The wave field breaks up in this case into a set of packets that are correlated in phase space  $(x, v_{ph})$ , while the particle phase trajectories form partially ordered streams in phase space. The turbulence-ordering process also leads to granulation of the distribution function and to noticeable deviation of the beam relaxation from quasilinearity. One of the remarkable results of the theory, confirmed by numerical experiments,<sup>8,9,11,12</sup> is the prediction that the initial field correlations are enhanced when beams with velocity spreads relax. We note that correlation phenomena accompanying beam relaxation were observed also in earlier numerical experiments.<sup>13,14</sup> It is also mentioned in recent communications,<sup>15,16</sup> on the basis of a theoretical analysis and of results of numerical modeling, that an important role is played by field and particle-motion correlations that lead to noticeable deviations from the predictions of the quasilinear approximation at

$$\tau_{NL} < \tau_{QL}.$$

We note while the estimates of the role of correlations in turbulent relaxation of beams have some com-

mon features, the theoretical models and the results exhibit substantial differences.<sup>1-4,7-12,13</sup> This circumstance makes particularly valuable the laboratory experiments that can check on the validity of various theoretical premises and of results of numerical modeling results in which one-dimensional models are used.

The validity of the quasilinear theory and of its predictions were experimentally verified most fully by Roberson and Gentle,<sup>17</sup> who studied the relaxation of a beam with a weak velocity spread placed in a longitudinal magnetic field. At very weak beam currents, good agreement with the quasilinear theory was obtained. An insignificant increase of the beam current, however, showed a decrease of the integrated energy of the wave field after the maximum was reached, and the appearance of a tail of accelerated particles on the beam distribution function. These deviations from the quasilinear-theory predictions were not investigated in detail.

Experimental result of a study of the relaxation of a monoenergetic electron beam in a plasma<sup>18,19</sup> have likewise a direct bearing on the discussed group of phenomena. The rapid hydrodynamic stage of beam relaxation, during which a narrow spectrum of resonant waves is excited, should give way to a quasilinear stage, in which the beam velocity spread  $\Delta v_b$  becomes substantial, i.e.,  $\Delta v_b/v_b \geq \gamma/\omega$ , where  $\gamma$  is the beam-instability growth rate. Indeed, in the experiments the spectrum of the excited waves turns out to be quite broad, and the smearing of the averaged velocity distribution function is large and reminiscent of a plateau. Yet an analysis of the structure of the field and of the particle distribution function has shown that the field consists of extended coherent repeating packets, and the beam distribution function is significantly granulated. The results show that during the later stage of relaxation of a monoenergetic beam not only are the long-lived macroparticles predicted by the theory<sup>1-3</sup> produced, but substantial correlations of the wave field are also preserved.

The correlation phenomena and their role in the process of relaxation of velocity-smearred beams have so far been very little investigated in laboratory ex-

periments. We report here the results of an experimental study of the indicated group of problems. A preliminary report on some of the results was published before.<sup>20</sup>

Before we proceed to the exposition of the experimental result, we list briefly the main properties of the quasilinear and partially ordered (moderately turbulent) relaxation process that is the subject of the experimental verification. Beam relaxation is referred to as quasilinear if the growth rates are much smaller than the frequencies,  $\gamma_h/\omega_h \ll 1$ , and the particle velocity spread  $\Delta v_b$  is large enough:

$$\bar{k}\Delta v_b \gg \gamma_h, \quad (1)$$

where  $\bar{k}$  is the average wave number of the unstable waves. It is necessary, in addition, that the quasilinear diffusion rate be low, so that during a time interval  $\tau_{QL} \sim \gamma_{QL}^{-1}$  the particle velocity does not manage to change by an amount  $\sim v_b$ . This condition can be expressed in the form

$$\bar{k}\Delta v_b \gg \Omega_{ir}, \quad \Omega_{ir} = (eE\bar{k}/m)^{1/2}. \quad (2)$$

Here  $\Omega_{ir}$  is the oscillation frequency of the resonant particles in the field of a wave of amplitude  $E = (8\pi W)^{1/2}$ , where  $W$  is the oscillation energy density.

The main properties of the quasilinear process are the following.

1) The amplitudes of the waves excited by the beam and the total energy of the oscillations are non-decreasing functions of the time, i.e.,  $\gamma_h(t) \geq 0$ , with  $\gamma_h(t) \rightarrow 0$  as  $t \rightarrow \infty$ .

2) The correlations of the wave field and of the particle motion do not play an essential role, and the correlation time is the shortest of all the characteristic times. This means that the initial correlations should disappear in time, so that asymptotically at  $t > \gamma_{QL}^{-1}$  the process does not depend on the initial conditions.

3) The particle distribution function spreads out diffusely in the region where its derivative  $\partial f/\partial v$  is positive, until a plateau is formed, so that in the saturation region  $\partial f/\partial v < 0$  for all  $v$ .

It was shown earlier<sup>8</sup> (see also Refs. 9–12) that to realize a quasilinear relaxation process a condition stronger than (2) must be satisfied, namely

$$\begin{aligned} \Omega_{ir}(k\lambda) &\ll \gamma_h, \\ (k^2 D_{QL})^{1/3} &\ll \gamma_h, \end{aligned} \quad (3)$$

where  $D_{QL}$  is the coefficient of quasilinear diffusion. The need to satisfy condition (3) if the quasilinear approximation is to hold has been demonstrated also in Ref. 15.

When condition (3) is violated, i.e., at  $\Omega_{ir} \sim \gamma_h$ , field correlations that ensure formation of ordered convective fluxes in phase space appear and become enhanced.<sup>6–12</sup> The quasilinear relaxation process is replaced by a partially ordered moderately turbulent process.

The following properties characterize the moderately turbulent relaxation stage.

1) The wave field breaks up into coherent packets

whose spatial dimensions  $l(\bar{v}_{ph})$  are connected with the amplitudes  $E(\bar{v}_{ph})$  by the relation

$$l(\bar{v}_{ph}) = l_{irr} = \pi \bar{v}_{ph} / \Omega_{ir},$$

where  $\bar{v}_{ph}$  is the average phase velocity of the packet.

2) The interaction of the packets via the resonant particles produces a mutual ordering of the packets in  $(x, v_{ph})$  space. We point out that the fact that the wave phase correlations become stronger rather than weaker means that the relaxation process becomes sensitive to the initial conditions, particularly to the initial correlations of the field.

3) As a result of the mutual ordering of the wave packets, the correlations of the motion of the trapped particles with spread of the initial phase coordinates

$$\Delta x < 2\pi/\bar{k}, \quad \Delta v < v_{tr} = 2(eE/m\bar{k})^{1/2}$$

are preserved in a time interval

$$\tau_{mix} \approx \tau_{QL}/2(1-w). \quad (4)$$

During this time, the particle velocity manages to change by an amount

$$\Delta v_{mix} = \frac{v_{tr}}{2} \left( 1 + \frac{w}{1-w} \xi \right). \quad (5)$$

In these relations,  $w$  is the ordering parameter,  $\frac{1}{2} \leq w \leq 1$ ;  $\xi$  is a quantity close to unity at  $\Omega_{ir} \gg \gamma_{QL}$  (see Ref. 12). The quantity  $v_{mix}$  plays the role of the phase-flux mixing "length."

4) A consequence of the phase-flux ordering is an increase of the growth rate of the packet amplitudes:

$$\gamma \approx \frac{v_{mix}}{v_{tr}} \gamma_{QL}. \quad (6)$$

5) The inhomogeneity of the distribution function is defined by the relation

$$|f - \bar{f}| \approx v_{mix} \frac{\partial \bar{f}}{\partial v}, \quad (7)$$

where  $\bar{f}(v)$  is the distribution function averaged over  $x$ .

6) The energy exchange between the particles and the waves is nonmonotonic, so that the growth rates  $\gamma_h$  can reverse sign. As for the total energy of the waves excited by a velocity-smear beam, its change can also be oscillatory if  $v_{mix}$  becomes comparable with the particle-velocity spread in the beam.

The experimental setup, the physical parameters of the beam-plasma system, and the conditions under which the experiment was performed are contained in Sec. 1. Section 2 is devoted to an investigation of the stability of the quasilinear relaxation process. In Sec. 3 are reported the experimental data on the evolution of weak coherent signals. The results of the study of the mechanism of the beam-enhanced wave packets are given in Sec. 4. The overall results are discussed briefly in Sec. 5.

## 1. EXPERIMENT

The experiments were performed with the setup illustrated in Fig. 1. It consists of a vacuum chamber 1 of 20 cm diam in which waveguide 2 of 15 cm diam

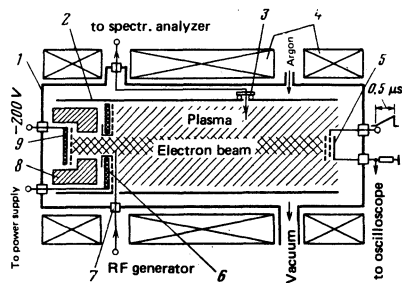


FIG. 1. Experimental setup. 1) Vacuum chamber, 2) waveguide, 3) moving carriage, 4) magnetic-field coils, 5) electrostatic analyzer, 6) plasma source, 7) RF antenna, 8) magnetic screen, 9) electron gun.

and 160 cm length is placed. A longitudinal slit along a waveguide generatrix serves as an entry for Langmuir and high-frequency (RF) probes as well as an electrostatic analyzer. Carriage 3 moves these units along the setup. A special unit transmits the rotation into the vacuum and converts it into the longitudinal carriage motion. An iris diaphragm can vary smoothly the diameter of the plasma column during the experiment from 2 to 15 cm. The vacuum chamber, the waveguide, and the other units are made of stainless steel. The setup was evacuated with an AVED-2M electric-arc titanium pump to a pressure  $10^{-7}$  Torr. The working gas was argon at a pressure  $10^{-5}$  Torr.

A uniform magnetic field up to 3 kOe was produced by a solenoid consisting of seventeen continuously operating segments 4. The length of the uniform section of the magnetic field was 150 cm.

The experiments were performed in a plasma of density  $n = 10^8 - 10^9 \text{ cm}^{-3}$  and electron temperature  $T_e = 1 - 5 \text{ eV}$  in a magnetic field  $H_0 = 1.5 \text{ kOe}$ . The length of the homogeneous section of the plasma column was 150 cm. The plasma was produced either by a cyclotron-resonance plasma source<sup>6</sup> of frequency  $\nu = 2400 \text{ MHz}$ , or a source based on a large-diameter diode gun.

The beam with longitudinal-velocity spread was produced by diode gun 9 (cathode diameter 0.8 cm) placed in a magnetic screen 8. The magnetic screen introduces a large magnetic-field inhomogeneity, in which the beam-electron velocities are effectively restructured. At one at the same total energy, the beam acquires a longitudinal-velocity spread, and it is only this velocity which determines the phenomena investigated by us. The plasma source and the electron gun are coaxially placed at one end of the setup. To prevent the electric fields of the plasma source from affecting the electron-beam distribution function, the beam was screened by electrostatic shields and by the channel through which the beam drifted through the source. The experiments were performed at beam currents 1.5–5 mA and energies 300–500 eV.

The beam distribution function was measured by a multigrad electrostatic analyzer 5 placed at the end of the setup. The circuit that included the analyzer could measure the time-averaged distribution function, as well as perform a rapid analysis of the beam within a time  $\tau \leq 500 \text{ nsec}$ . The time-averaged distribution

function was automatically recorded in  $F(v)$  coordinates as a function of the longitudinal energy and then converted into a function of the longitudinal velocity. The differentiation of the collector current with respect to the analyzer blocking potential was produced by an electric circuit with a transformer and an SD-1 synchronous detector. In the case of the fast analysis, an S1-31 oscilloscope was used to record the collector current as a function of the voltage on the analyzer blocking grid, followed by numerical integration of the current.

The parameters of the plasma and of the oscillation are recorded by a system of movable and immobile RF probes in conjunction with broadband amplifiers and oscilloscopes. The initial bare monochromatic wave was excited by antenna 7 as the beam entered the plasma. When an oscillation packet was fed into the system, a special synchronization circuit switched over the high-frequency oscillator to operate in an external-modulation regime.

## 2. DEPENDENCE OF RELAXATION PROCESS ON THE BEAM CURRENT

In this section we study the effect exerted on the beam relaxation by a change in the beam-electron density  $n_b$  at a fixed electron velocity distribution. We measured in this case the time-averaged beam distribution function  $f(v)$  as well as the integrated oscillation power  $W(z)$  and power spectrum  $P(\nu, z)$  as functions of the distance  $z$ . The dispersion curve, determined by measuring the wavelength as a function of the frequency, shows that a fundamental radially symmetrical magnetized-plasma space-charge wave-potential mode is excited in the experiment.

The evolution of the integrated power  $W(z)$  along the system, for a beam current  $I \leq 2 \text{ mA}$ , is shown in Fig. 2, curve 1. The exponential growth of  $W(z)$  gives way to a slower one, reaching a maximum at  $z = z_m = 135 \text{ cm}$ . The beam distribution function flattens out then into a plateau (Fig. 3, curve 2) followed in the high-energy region by a descending section. The maximum energy of the particles in the relaxed beam is the same as in the injected beam. Thus, at a current  $I \leq 2 \text{ mA}$  we observe a typical picture of quasilinear relaxation.

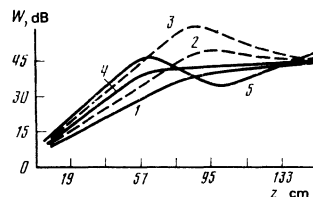


FIG. 2. Integrated noise power vs. length for various beam currents (curves 1–3) and initial coherent signals (curves 4 and 5). 1)  $I = 1.8 \text{ mA}$ , 2)  $2.4 \text{ mA}$ , 3)  $2.8 \text{ mA}$ , 4)  $1.8 \text{ mA}$  (coherent signal at 72 MHz frequency as an initial amplitude five times larger than the noise amplitude at the same frequency; final signal amplitude 35 dB higher than initial); 5)  $I = 1.8 \text{ mA}$  (coherent signal at 72 MHz with amplitude 3 times larger than in case 4).

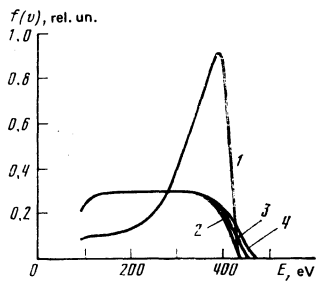


FIG. 3. Distribution functions of beam at various beam currents: 1) Initial, 2)  $I = 1.8$  mA; 3) 2.4 mA, 4) 2.8 mA.

The relaxation has a different character when the beam current is increased somewhat. At  $I = 2.4$  mA (Fig. 2, curve 2)  $W(z)$  increases exponentially during the initial stage, with a growth rate approximately 1.2 times larger than at  $I = 2$  mA. At a distance  $z = z(I) = 90$  cm, however,  $W(z)$  reaches a maximum and begins to decrease. The beam distribution function, just as at  $I \leq 2$  mA, has a plateau, but also a tail of accelerated particles whose energies reach 450 eV (Fig. 3, curve 3). The distance at which  $W(z)$  reaches its maximum at  $I = 2.4$  mA is smaller by a factor 1.4 than at  $I = 2$  mA. It is seen therefore that when the beam current is increased the particle transport velocity is higher than in quasilinear diffusion.

With further increase of the beam density, the growth rate of  $W(z)$  increases is proportion to  $n_b$ ; the function  $W(z)$  reaches its maximum at a shorter distance,  $z(I) = 80$  cm at  $I = 2.8$  mA, followed by a rapid decrease of  $W(z)$ , which recalls the oscillations of  $W$  in a relaxing monoenergetic beam (Fig. 2, curve 3). The tail of the accelerated electrons also increases with increasing current, reaching an energy 475 eV (Fig. 3, curve 4).

The form of the spectral density of the beam-excited oscillations does not undergo significant changes with change of the beam current, but at  $I > 2$  mA the variation of the field amplitudes ceases to be monotonic, and the nonmonotonicity is more strongly pronounced than in the change of the integrated oscillation power.

Figure 4 shows plots of the measured growth rates of the waves belonging to different sections of the spectrum vs. the length of the system at a beam current  $I > 2$  mA. The spatial increments were calculated from the formula  $\gamma = N/8.6z$ , where  $N = 20 \log(E1/E2)$  is the beam gain in dB, and  $z$  is the distance from the

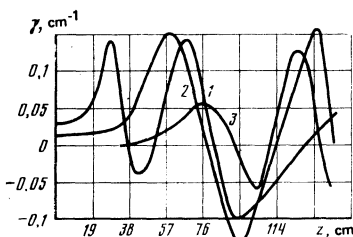


FIG. 4. Dependence of spatial growth rate on the length for waves with frequencies: 1)  $\nu = 40$  MHz, 2) 72 MHz, 3) 95 MHz at a beam current  $I = 2.4$  mA.

entry of the beam into the plasma, in centimeters. At a current  $I \leq 2$  mA the wave growth rates vary little with the length at first, then increase by 2–3 times, after which they decrease and tend to zero (see Fig. 4a of Ref. 20). At  $I > 2$  mA the growth rates begin to oscillate over the length and take on both positive and negative values (Fig. 4).

It is seen from an examination of the results that at  $I > 2$  mA the beam-relaxation process differs qualitatively from quasilinear. The accelerated energy exchange between the particles and the waves and the reversible character of this process point to the presence of correlations between the field and the particle motion. The formation of coherent wave packets can be easily discerned from the plots of the potential oscillations at large distance from the entry; coherent packets appear predominantly at low frequencies both at  $I \leq 2$  mA and at larger currents, but at  $I \geq 2$  mA they are much more frequently encountered. No quantitative reduction was made of the plots of the potential oscillations.

A packet with amplitude  $E$  and average phase velocity  $\bar{v}_{ph}$  can accelerate trapped particles to velocities  $v = \bar{v}_{ph} + 2(E/mk)^{1/2}$  if the packet length  $l > l_{int} = \pi \bar{v}_{ph} / \Omega_{tr}$ . It is precisely this process which causes the appearance of fast particles.<sup>1)</sup>

### 3. INFLUENCE OF INITIAL CORRELATIONS ON THE BEAM RELAXATION PROCESS

In the quasilinear approximation, owing to the diffuse character of the beam relaxation and to absence of interaction between the waves, the relaxation process is not sensitive variations of the initial conditions. However, if this approximation actually ceases to hold if conditions (2) is violated, when the correlation of the field and of the particle motion do not weaken but become stronger, then the initial conditions should play the decisive role in the character of the relaxation process.

We have investigated the effect of controllable initial field correlations on the relaxation of a beam with a weak current  $I = 1$  mA. To this end we applied to the input weak (with amplitudes much below saturation) periodic signals at frequencies located in the beam amplification band. It was observed that the initial correlations are not disturbed in the course of the relaxation, and influence this process significantly.

The evolution of the integrated power of the beam-excited oscillations  $W$  depends essentially on the amplitude of the initial signal (Fig. 2, curves 1, 4, and 5). Although  $W$  saturates independently of the initial signal  $W$  at approximately the same asymptotic value (curve 4), the average growth rate is larger in the presence of a coherent signal and increases with increasing amplitude  $A$  of the latter. If it is assumed that at  $A = 0$  the average growth rate has the quasilinear value  $\gamma_{QL}$ , then at  $A \neq 0$  the growth rate (which shall call moderately turbulent) exceeds the quasilinear value,  $\gamma_{tb}^{(1)} \approx 1.4 \gamma_{QL}$  for the case represented by curve 4 of Fig. 2, and  $\gamma_{tb}^{(2)} \approx 1.7 \gamma_{QL}$  for the case of curve 5 of Fig.

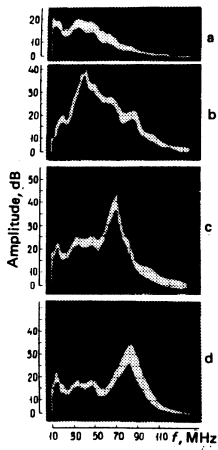


FIG. 5. Noise spectrum at length  $z = 76$  cm: a) in the absence of a coherent signal; coherent signal is present at the following frequencies: b)  $\nu = 40$  MHz, c) 71 MHz, d) 89 MHz. The coherent signals have an initial amplitude five times larger than the noise amplitude at the same frequencies. The final signal amplitudes are 30–40 dB higher than the initial ones.

2. Hence, using relations (3) and (6), we can estimate the particle-motion correlation length in  $v$  for both cases:

$$v_{\text{mix}}^{(1)} \approx 1.4v_{tr}, \quad v_{\text{mix}}^{(2)} \approx 1.7v_{tr}.$$

An increase of the amplitude of the initial perturbation (Fig. 2, curve 5) is accompanied by a qualitative change in the behavior of the integrated noise-spectrum power along the setup: in addition to a maximum, its distribution shows a nonmonotonicity similar to that observed at  $I > 2$  mA (see Sec. 2).

Both as in the absence of an initial coherent signal and in its presence, the beam distribution function becomes flat-topped in the course of the relaxation. At low initial-signal amplitudes  $A$  (not more than 5 times larger than the noise level at the input) no tail of accelerated particles is observed on the beam distribution function at the far end of the setup. At values of  $A$  more than 5 times the initial-noise level, accelerated particles appear and their percentage increases with increasing  $A$ .

The most substantial manifestation of the initial correlations is observed in the evolution of the oscillation spectrum. Figure 5 shows the spectra of the beam-amplified waves in the absence of an initial coherent signal (Fig. 5a) and in its presence (Figs. 5b–5d) for three input-signal frequencies  $\nu = 35$ , 72, and 89 MHz, obtained at a distance  $z = 76$  cm (the initial level of the signals at all these frequencies was 5 times the noise level). Only at the entrance end of the setup can one see a narrow line at the modulation frequency. The line broadens with increasing frequency (Figs. 5b–5d) and forms a packet of waves in the vicinity of the modulation frequency. The width of the packet, according to preliminary estimates, is approximately  $\Omega_{tr}$ .

The results offer evidence that the initial correlations are not disturbed in the course of the beam relaxation

and influence substantially this process even in the case of weak currents, when there are no visible manifestations of correlation phenomena in the behavior of  $W(z)$  and  $f(v, z)$ .

#### 4. INVESTIGATION OF THE MECHANISM OF INTERACTION OF WAVES AMPLIFIED BY A SMEARED BEAM

The results of the preceding sections attest to the onset of field correlation (formation of coherent packets) and particle-motion correlation (formation of tails of accelerated particles and acceleration of the energy exchange between the waves and the particles). It is of interest to investigate in greater detail the mechanism of the interaction of the waves with the resonant particles and with one another via resonant particles, since this mechanism produces the observed correlations. To study this question we used a system with so weak a beam current that no relaxation of the latter could be established over the length of the apparatus, i.e., there were no noticeable distortions of the beam distribution function or enhancement of the field by the beam on the far end of the apparatus. A packet of small-amplitude oscillations was fed into the entry of this system from the outside; the spectral components of the packet were located inside the beam amplification band. Such an oscillation packet was significantly enhanced as it propagated along the system. In the absence of substantial interactions of the waves with one another via resonant packet, the packet should undergo a weak amplification (as well as fluctuations) as it propagates along the system. Its shape should be weakly changed at the same time. Our results reveal considerable deviations from such a picture.

Figure 6 shows the evolution of two-plasma-wave packets excited at the input, with different carrier frequencies,  $\nu = 50$  and  $\nu = 90$  MHz. The figure shows the time scans of the oscillations recorded by a probe at various distances from the input antenna. The dashed lines determine the locations of packets moving with the initial group velocities. As seen from the figure, the group velocities of the packets are different. The dispersion of the field is such that for the  $\nu = 50$  MHz packet the group and phase velocities are close (long-wave packet), whereas at  $\nu = 90$  MHz these velocities are different,  $v_{gr} < v_{ph}$  (short-wave packet). Even though the initial fluctuations are not greatly amplified, the amplitudes of the excited packets, increasing exponentially, reach saturation and then begin

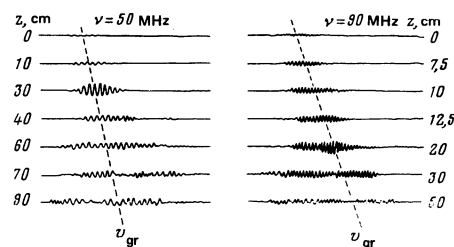


FIG. 6. Evolution of two plasma-wave packets along the length of the setup.  $v_{gr} \approx v_{ph}$  for the carrier  $\nu = 50$  MHz and  $v_{gr} < v_{ph}$  for  $\nu = 90$  MHz.

to decrease. The packet with the  $\nu = 50$  MHz carrier reaches a maximum amplitude at  $z = 30$  cm, and the one with  $\nu = 90$  MHz at  $z = 20$  cm. Beyond these distances, the packet evolution shows one more characteristic feature: the length of each packet increases, because they acquire precursors and tails with characteristic frequencies other than the initial one. In addition, amplitude-phase modulation of the packets is observed.

For the packet with  $\nu = 50$  MHz, a shorter-wavelength tail always follows the main packet at  $z \geq 40$  cm. The wavelength of the priming packet is noticeably shorter for the 90 MHz packet than at 50 MHz, and precursors and a tail appear almost simultaneously at  $z > 20$ . With further evolution of the group of packets, the amplitudes of the precursor and of the tail increase rapidly, the length of each of them increases, and substantial amplitude modulation sets in at  $z > 25$  cm.

It is also seen from the figure that the initial small-amplitude packet is transformed into a complete system of plasma-wave packets that interact with one another and have velocities both higher and lower than the initial packets. Although the waves are unstable in a large phase-velocity interval, the fact that new packets are produced near the priming one is evidence that the initial packet enhances the instability of the neighboring (in terms of the phase velocities) waves by perturbing the distribution function of the resonant particles. This phenomenon is possible only if the correlations of the particle motion in the amplified waves are preserved for a long time.

Figure 7 shows plots of the amplitudes of the initial packets (curves 1 and 1'), of the amplitudes of the new short-wave packets that lag the main ones (curves 2 and 2') and of the amplitudes of the long-wave packets that overtake the main ones (curves 3 and 3'), in relative units, along the system for the respective frequencies 90 and 50 MHz. In both cases it is seen that the exponential stage of the growth of the main packet gives way to a stage of saturation and damping, with excitation of precursors and tails. The main-packet amplitude threshold of excitation of new plasma-wave packets is clearly seen. With increasing amplitudes of the new packets, the amplitude of the main packet drops to values lower than the amplitudes of the new packets.

Figure 8 shows beam distribution functions measured

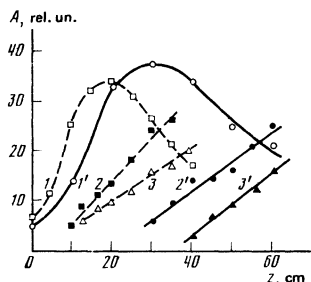


FIG. 7. Dependence of the amplitude of the main packet (curves 1 and 1'), the lagging packet (2 and 2'), and the overtaking packet (curves 3 and 3') along  $z$  for packets with carriers  $\nu = 90$  MHz (dashed curves) and  $\nu = 50$  MHz (solid).

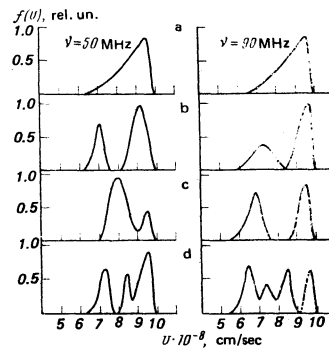


FIG. 8. Distribution function at far end of setup vs. the amplitude  $A$  of the initial packets: a)  $A = 0$ , b)  $A = 0.3$  V, c) 1.0 V, d) 5 V. Measurement time  $\tau = \text{nsec}$ .

for a short time on the far end of the system at different amplitudes of the initial packet. The initial distribution function increases monotonically with increasing velocity, and has an appreciable velocity spread (Fig. 8a).

The presence of an initial packet with amplitude  $A = 0.3$  V leads to formation of a double-hump structure (Fig. 8b). With increasing amplitude of the initial packet (Figs. 8c and 8d) a nonmonotonic "spike" structure is observed on the distribution functions and attests to the onset of correlated groups of particles. Measurements show that the nonmonotonic spike structure has a characteristic velocity scale  $\Delta v \sim (2eE/mk)^{1/2}$ . We note that a similar structure of the distribution of an initially monoenergetic beam was observed earlier.<sup>19</sup>

Our investigations, on the one hand, confirm once more that the initial correlations influence substantially the character and rate of the relaxation of a smeared beam, and on the other hand reveal wave interaction via resonant particles. It is this interaction which ensures the establishment of the correlations of the field and of the particle motion, as seen from an analysis of the oscillations of the potential and of the particle velocity distribution function.

## 5. DISCUSSION OF RESULTS

Our investigations show that the diffusion relaxation of a beam with a velocity spread is disturbed both when the instability margin (beam density) is increased, and when initial field correlations are present. It is probable that the turbulent convection of the particles in velocity takes place also at small ( $I < 2$  mA) beam currents, but since the mixing length  $v_{\text{mix}}$  remains negligibly small compared with the velocity spread of the particles, this can lead only to a renormalization of the diffusion coefficient and of the growth rates which, judging from the results of the theory and of the numerical experiments,<sup>8-12</sup> cannot differ greatly from the quasilinear values. The most important conclusion, in our opinion, is that despite the broad oscillation spectrum and the large velocity spread in the beam, the initial correlations are not disturbed in the course of the relaxation, and influence substantially this very process.

The use of controllable initial correlations has enabled us to establish that during a later stage of the relaxation there are actually formed coherent wave packets with characteristic frequency width  $\Delta\omega \sim \Omega_{tr}$ , and that, furthermore, the field correlations give rise to a regime of turbulent convection of the particle phase trajectories, with a characteristic mixing length exceeding  $v_{tr}$ , thus leading to an increase of the growth rates, to the appearance of reversible energy exchange between the waves and the particles, and to tails of fast particles with velocities exceeding the maximum velocity of the injected beam.

The interaction of the waves with the resonant particles and with one another via resonant particles can be observed in pure form by amplifying the priming oscillation packets by a weak beam. We note that the evolution of large-amplitude packets with spatial dimension  $l \sim l_{int} = v_{ph}/\Omega_{tr}$  at a stable initial distribution function was investigated earlier by numerical modeling<sup>22</sup> and in a laboratory experiment (Ref. 23).<sup>23</sup> There, too, they succeeded in observing broadening of the packet on account of the appearance of precursors and tails excited by resonant particles whose distribution function was modulated by interaction with the main packet. The phase velocities of the precursor and of the tail also differed from the average phase velocity of the main packet. The distinguishing feature of our case is the instability of the initial distribution function, which leads on the average to amplification of the interacting packets. The character of the evolution of the profiles and amplitudes of the packets agrees with the theoretical description of the evolution of beam-enhanced packets of space-charge waves,<sup>26</sup> an experimental study of which was initiated earlier.<sup>27</sup>

The spiked distribution of the beam-particle velocities is evidence of formation of large ( $\Delta v \sim v_{tr}$ ) macro-particles and of their convective transport in phase space.

Comparing the experimental results with the main predictions of the quasilinear theory and of the theory of moderate turbulence (see the introduction), we see that the latter is valid. Quasilinear relaxation can take place for rather weak beams and in the absence of considerable initial field correlations. It appears that this process might be realized also under initial conditions of more general form if the system were to contain additional mixing factors that lead to randomization of the wave phases and to stochastization of the particle motion.

The authors thank K. N. Stepanov for support and helpful remarks, Yu. S. Sigov for a discussion of the results, and V. I. Zinchenko for help with the experiments.

<sup>1)</sup> A recent paper<sup>21</sup> reports an experimental study of the mechanism of formation of accelerated particle in the course of beam relaxation under similar conditions.

<sup>2)</sup> A theoretical treatment of the evolution of long packets ( $l \gg l_{int}$ ) is contained in Refs. 24 and 25.

- <sup>3)</sup> B. B. Kadomtsev and O. P. Pogutse, Phys. Rev. Lett. **25**, 1155 (1970); Report IC/70/54, Int. Centre for Theor. Phys., Trieste, 1970. Proc. Europ. Conf. Control. Fusion Plasma, Phys., Rome, 1970, p. 74.
- <sup>4)</sup> B. B. Kadomtsev and O. P. Pogutse, Phys. Fluids **14**, 2470 (1971).
- <sup>5)</sup> T. H. Dupree, Phys. Rev. Lett. **25**, 789 (1970).
- <sup>6)</sup> T. H. Dupree, Phys. Fluids **15**, 334 (1972).
- <sup>7)</sup> A. A. Vedenov, E. P. Velikhov, and R. Z. Sagdeev, Nuclear Fusion **1**, 82 (1961).
- <sup>8)</sup> W. E. Drummond and D. Pines, Nuclear Fusion Suppl. **3**, 1049 (1962).
- <sup>9)</sup> J. H. Misquich and R. Balescu, Plasma Phys. **20**, 781 (1978).
- <sup>10)</sup> A. S. Bakai, Dokl. Akad. Nauk SSSR **237**, 1069 (1977) [Sov. Phys. Dokl. **22** 753 (1977)].
- <sup>11)</sup> A. S. Bakai and Yu. S. Sigov, *ibid.* **137**, 1326 (1977) [**22**, 734 (1977)].
- <sup>12)</sup> A. S. Bakai and Yu. S. Sigov, Preprint No. 52, IPM AN SSSR (Inst. Prob. of Mech., USSR Acad. Sci.), 1977.
- <sup>13)</sup> A. S. Bakai and Yu. S. Sigov, Preprint No. 34, IPM AN SSSR, 1978.
- <sup>14)</sup> A. S. Bakai, 7th Internat. Conf. on Plasma Phys. and Cont. Nuclear Fusion Research, Innsbruck, Austria, 23-30 August 1978. Conf. Proc. Rep. Nx-4-2, 1979, Vol. III.
- <sup>15)</sup> R. Morse and C. Nielson, Phys. Fluids **12**, 2418 (1969).
- <sup>16)</sup> D. Biskamp and H. Welter, Nuclear Fusion **12**, 89 (1972).
- <sup>17)</sup> J. C. Adam, G. Laval, and D. Pesme, Phys. Rev. Lett. **43**, 1671 (1979).
- <sup>18)</sup> J. C. Adam, G. Laval, and D. Pesme, 14th Int. Conf. on Ionized Phen. in Gases, Grenoble, 1979. Rep. NC-7-671, p. 671.
- <sup>19)</sup> C. Roberson and K. W. Gentle, Phys. Fluids **14**, 2461 (1971).
- <sup>20)</sup> V. A. Lavrovskii, I. F. Kharchenko, V. M. Deev, S. A. Rogashkov and Yu. G. Yaremenko, Zh. Tekh. Fiz. **39**, 1586 (1969) [Sov. Phys. Tech. Phys. **14**, 1190 (1970)].
- <sup>21)</sup> V. A. Lavrovskii, I. F. Kharchenko, and E. G. Shustin, Zh. Eksp. Teor. Fiz. **65**, 2236 (1973) [Sov. Phys. JETP **38**, 1117 (1974)].
- <sup>22)</sup> A. S. Bakai, S. M. Krivoruchko, and S. A. Nekrashevich, Pis'ma Zh. Eksp. Teor. Fiz. **29**, 577 (1979) [JETP Lett. **29**, 526 (1977)].
- <sup>23)</sup> K. B. Freese, J. E. Walsh, and J. Lohr, Phys. Fluids **22**, 2367 (1979).
- <sup>24)</sup> J. Denavit and R. N. Sudan, Phys. Rev. Lett. **28**, 404 (1972).
- <sup>25)</sup> N. Sato, K. Saeki, and R. Hatakeyama, Phys. Rev. Lett. **38**, 1480 (1977).
- <sup>26)</sup> D. D. Ryutov and V. N. Khudik, Zh. Eksp. Teor. Fiz. **64**, 1252 (1973) [Sov. Phys. JETP **37**, 637 (1973)].
- <sup>27)</sup> Ya. N. Istomin and V. I. Karpman, Zh. Eksp. Teor. Fiz. **63**, 131 (1972) [Sov. Phys. JETP **36**, 69 (1973)].
- <sup>28)</sup> A. S. Bakai and V. I. Maslov, All-Union Conf. on the Interaction of Electromagnetic Waves with Plasma, Dushanbe, 1977, Abstracts, p. 77.
- <sup>29)</sup> S. M. Krivoruchko, V. A. Bashko, and A. S. Bakai *ibid.* p. 67.

Translated by J. G. Adashko